Modeling and Control of a Marine Diesel Engine driving a Synchronous machine and a Propeller*

Mutaz Tuffaha † and Jan Tommy Gravdahl ‡

Abstract

In some designs of power systems for marine vessels, large-size or medium-size Diesel engine(s) is(are) used to drive one synchronous machine to generate electricity, and the main propeller, simultaneously, through a gear box. Such systems are subject to disturbances that may affect performance and fuel consumption. The most important disturbances occur due to the propeller torque, and load demand on the electric network. In this work, a simplified state-space model is suggested for such systems based on well known models of each component. The model considers the dynamics of the shaft, Diesel engine, and synchronous machine with the propeller in their simplest models. The output voltage and torque coefficient were modeled as uncertain parameters. Then, exploiting feedback linearization, two controllers were suggested for the proposed model to regulate the rotational speed of the shaft. Firstly, by pole placement. The second is a robust controller by mixed H_2/H_∞ synthesis. The results of the simulations of the proposed controller are presented and compared.

1. INTRODUCTION

The power systems on marine vessels take many configurations and designs according to their purposes, and size. Companies in the field contend for designing and manufacturing better systems regarding efficiency, reliability, fuel saving, and environmental friendliness. The Diesel engine is most commonly used due to its efficiency, and low cost [1]. The propellers are driven either electrically (by a motor of any type), or mechanically (e.g. a Diesel engine) [2], [3]. In both cases, Diesel engines are needed aboard to drive synchronous machines to generate electricity. Lately, the control of *Diesel Generating Set* (Genset) has become one of the most important and indispensable topics in the field. The authors in [4] noted that the air dynamics of the turbo-charger may lead to undesired oscillations in the speed of the prime mover in power plants driven by Diesel engines. Hence, they suggested an adaptive controller to remedy these oscillatory dynamics [4]. Spurred by environmental reasons and the urge to save fuel, some systems, that have been developed for marine vessels recently, comprise propellers that can be driven mechanically and/or electrically. Such designs exploit large or medium-size diesel engine(s) that can drive both the main propeller, and synchronous machine as shown in Fig. 1. The synchronous machine in such designs works either as a motor or as a generator. When the machine is driven by the electric power from the bus as a motor, it is described as *Power-Take-In* (PTI), whereas when it is driven by the mechanical power produced by the diesel engine to generate electric power, it is described as *Power-Take-Out* (PTO). Hence, the system operate in several modes, and can be considered as a *Hybrid system*.

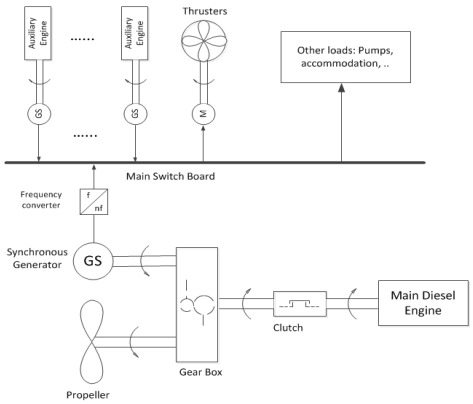

Figure 1: Schematic of the main network of the power systems on board subject of research.

To the authors best knowledge, systems like the one in Fig. 1 have not been treated in the control literature as one system due to its complexity. The complexity

*This work was sponsored by Norwegian Research Council and SINTEF Fisheries and Aquaculture through the ImproVEDO-project

†M. Tuffaha is with the Department of Engineering Cybernetics, Faculty of Information Technology, Mathematics and Electrical Engineering, Norwegian University of Science and Technology, NO-7491 Trondheim, Norway mutaz.Tuffaha@itk.ntnu.no

‡J. T. Gravdahl is with the Department of Engineering Cybernetics, Faculty of Information Technology, Mathematics and Electrical Engineering, Norwegian University of Science and Technology, NO-7491 Trondheim, Norway jan.tommy.gravdahl@itk.ntnu.no

of the system arises from the fact that the propeller can be driven electrically, or mechanically. Most of the authors in this arena treat the two cases separately. For example, the authors in [5], and [6] proposed two different approaches to tackle the problem of controlling the Genset, but both of the works considered the propeller as part of the load since it is driven electrically. Our target, as a future work, is to put a model for this hybrid system in all modes of operation, then, design a supervisory power generation controller. However, as a first step, a simplified model is proposed for the above system in this work. Inasmuch as the system described is complicated, the following assumptions were made:

1. The synchronous machine is working in one mode, PTO.

2. The Diesel-engine is medium-size.

3. Low-level controllers are used to regulate the propeller torque, and output voltage of the generator.

Then, well known simplified models of each component of the system described were combined. The frequency converter is not included in the model as it is presumed that regulating the shaft speed of the synchronous machine guarantees that the fluctuations in frequency could be handled by the low level controllers of the converter. The output voltage and torque coefficient were modeled as uncertain parameters. Then, due to its ability to handle disturbances, feedback linearization was exploited to design two different controllers for the proposed model to regulate the shaft speed. A controller by using the regular pole placement technique was proposed. Then, a mixed H_2/H_∞ controller was designed for its robustness against uncertainties, based on the strategy proposed in [7]. Simulations of the proposed model were performed with the two control techniques for comparison purposes.
The proposed model is developed in the next section. In the third section, the feedback linearization is applied to get a control law by pole placement. Then, the robust controller is presented. Section V presents the results of the simulations performed. Finally, some conclusions are drawn in the last section.

2. MATHEMATICAL MODEL

The shafts of the propeller, synchronous machine, and diesel engine are geared to each other, so before describing the mathematical model, let us define the notation used for the gearing effect. First, let R_{XY} denote the gear ratio between gear X and gear Y, such that:

$$R_{XY} = \frac{\Omega_X}{\Omega_Y}, \tag{1}$$

where Ω is the rotational speed in rad/sec. Note that $R_{XY} = \frac{1}{R_{YX}}$. Since the shafts are geared to each other, the rotational speeds can be related, according to (1), as:

$$\Omega_P = R_{PM}\Omega_M \tag{2a}$$
$$\Omega_E = R_{EM}\Omega_M, \tag{2b}$$

where the subscripts M, P, and E denote the machine, propeller, and diesel engine, respectively. The torque applied to (obtained from) any shaft will affect the angular acceleration of the other two shafts. Let $\mathscr{Q}$ be the torque applied or obtained. Let the sub subscript denote the side, e.g., $\mathscr{Q}_{E_M}$ denote the engine torque as seen from the machine side, then:

$$\mathscr{Q}_{E_M} = R_{EM}\mathscr{Q}_{E_E}, \tag{3}$$

and for simplicity, let $\mathscr{Q}_{E_E}$ be denoted by $\mathscr{Q}_E$.

2.1. Shaft Dynamics

The main diesel engine drives both the synchronous machine and the propeller. The torque applied by the engine on the shaft will accelerate all the shafts. Besides, there will be a counter torque on the propeller shaft, and the synchronous machine. Hence, the engine main shaft dynamics can be written as:

$$\begin{aligned}\mathscr{Q}_E &= R_{ME}J_M\dot{\Omega}_M + R_{PE}J_P\dot{\Omega}_P + \mathscr{Q}_{M_E} \\ &\quad + \mathscr{Q}_{P_E} + \mathscr{Q}_f \\ &= R_{ME}^2J_M\dot{\Omega}_E + R_{PE}^2J_P\dot{\Omega}_E + R_{ME}\mathscr{Q}_M \\ &\quad + R_{PE}\mathscr{Q}_P + \mathscr{Q}_f \\ &= (R_{ME}^2J_M + R_{PE}^2J_P)\dot{\Omega}_E + R_{ME}\mathscr{Q}_M \\ &\quad + R_{PE}\mathscr{Q}_P + \mathscr{Q}_f,\end{aligned} \tag{4}$$

where J_M is the moment of inertia of the machine and its shaft, J_P is the moment of inertia of the propeller, and its shaft. $\mathscr{Q}_f$ is the frictional torque. Alternatively, the dynamics of the engine shaft can be transferred to the machine side to get:

$$(J_M + R_{PM}^2J_P)\dot{\Omega}_M = R_{EM}\mathscr{Q}_E - \mathscr{Q}_M - R_{PM}\mathscr{Q}_P - \mathscr{Q}_f \tag{5}$$

2.2. Synchronous Machine Model

The synchronous generator model, in *per unit* (p.u.) notation, and in dq-frame, can be stated as [8]:

$$\psi_d = -X_di_d + X_{Fd}i_F \tag{6a}$$
$$\psi_q = -X_qi_q \tag{6b}$$
$$\psi_F = X_Fi_F - X_{Fd}i_d, \tag{6c}$$

and

$$0 = \omega_M\psi_q + u_d \tag{7a}$$
$$0 = -\omega_M\psi_d + u_q \tag{7b}$$
$$\dot{\psi}_F = \omega_0(-R_Fi_F + u_F), \tag{7c}$$

where ψ_d, ψ_q are the $d-$, and $q-$axis components of the stator flux linkages, respectively. u_d, and u_q are the $d-$, and $q-$axis components of the terminal voltage. i_d, and i_q are the $d-$, and $q-$axis components of the stator current. i_F, ψ_F and u_F are the field circuit current, flux linkage, and voltage, respectively. X_d, and X_q are the $d-$, and $q-$axis components of the stator self inductance. X_F, and R_F are the field circuit self inductance, and resistance, respectively. X_{Fd} is the mutual inductance between the field circuit and stator windings.

Moreover, ω_M is the rotational speed of the rotor in p.u., which is given by:

$$\omega_M = \frac{\Omega_M}{\Omega_{M_{base}}}, \tag{8}$$

where $\Omega_{M_{base}} = \frac{\omega_0}{(p/2)}$, with p the number of poles, and the nominal frequency $\omega_0 = 2\pi f_0$, as given in Table 1. Note that from (8), the p.u. values of the rotational speeds are equal since:

$$\begin{aligned} \omega_M &= \frac{\Omega_M}{\Omega_{M_{base}}} = \frac{R_{MP}\Omega_P}{R_{MP}\Omega_{P_{base}}} = \omega_P \\ &= \frac{R_{ME}\Omega_E}{R_{ME}\Omega_{E_{base}}} = \omega_E, \end{aligned}$$

where the base quantities are given in Table 2. Hence, from here on $\omega_M = \omega_P = \omega_E = \omega$.

It is worth noting, that damper windings, and stator resistance are neglected in (6), and (7), and so is stator flux dynamics (i.e., $\dot{\psi}_d = \dot{\psi}_q = 0$). After some algebraic simplifications, The equations (6), and (7) can be rearranged to give:

$$\dot{\psi}_F = \omega_0 \left[\frac{1}{\tau_F} \left(-\frac{X_d}{X'_d}\psi_F + \frac{X_{Fd}}{X'_d}\frac{u_q}{\omega} \right) + u_F \right], \tag{9}$$

where $\tau_F = \frac{X_F}{R_F}$ is a time constant and $X'_d = X_d - \frac{X^2_{Fd}}{X_F}$. The electromagnetic torque obtained from the machine in p.u. is given by (see [8]):

$$Q_M = \psi_d i_q - \psi_q i_d, \tag{10}$$

which can be rewritten by using (6), and (7) as:

$$Q_M = \left(\frac{1}{X_q} - \frac{1}{X'_d} \right) \frac{u_q u_d}{\omega^2} + \frac{X_{Fd}}{X_F X'_d}\frac{u_d \psi_F}{\omega}. \tag{11}$$

From here on Q denotes the torque in p.u., instead of the previous notation of $\mathscr{Q}$. Let $\delta = (\frac{p}{2})\Omega_M t - \omega_0 t + \delta_0$ be the angle between the rotor and a synchronously rotating reference as depicted in Fig. 2, then:

$$\dot{\delta} = \omega_0(\omega_M - 1). \tag{12}$$

Let U be the terminal voltage of the stator of the synchronous machine, then the terminal voltages in dq-frame would be, $u_d = U\sin\delta$, and $u_q = U\cos\delta$. Thus,(9), and (11) can be rewritten as:

$$\dot{\psi}_F = \frac{\omega_0}{\tau_F X'_d} \left(-X_d\psi_F + X_{Fd}\frac{U\cos\delta}{\omega} \right) + \omega_0 u_F, \tag{13}$$

and

$$Q_M = \left(\frac{1}{X_q} - \frac{1}{X'_d} \right) \frac{U^2\sin(2\delta)}{2\omega^2} + \frac{X_{Fd}}{X_F X'_d}\frac{U\psi_F\sin\delta}{\omega}. \tag{14}$$

2.3. Propeller Model

The propeller torque depends on the size and type of the propeller, and the operational mode of the vessel. The models can be complicated if more than one operational mode is considered. The propeller torque of the *fixed pitch propeller* (FPP) is modeled by [2], [3], and [9] as:

$$\mathscr{Q}_P = \rho D^5 K_Q n_P^2 \tag{15}$$

where $n_P = \frac{\Omega_P}{2\pi}$ is the rotational speed in rev/s, ρ is the density of water in Kg/m^3, D is the propeller diameter in m, and K_Q is the dimensionless propeller torque coefficient. The coefficient K_Q depends on the *advance ratio* (J), which in turn depends on the *advance speed* (u_a). Many models have been suggested in literature to model the torque coefficient K_Q and describe its dependence on J, and u_a, see e.g. [2], and [3]. In this work, we suggest considering K_Q as an uncertain parameter. To justify, propeller torque is usually controlled by multi-level controllers that are beyond the scope of this work. Our target is to investigate the ability to regulate the rotational speed of the described system regardless of the propeller torque variation. Thus, accepting the aforementioned argument, the model above can be described, in p.u., as:

$$\begin{aligned} Q_P &= \frac{\rho D^5}{Q_{P_{base}}} K_Q n_P^2 \\ &= \frac{\rho D^5}{4\pi^2 Q_{P_{base}}} K_Q \Omega_P^2. \end{aligned} \tag{16}$$

Inserting (1), and (2) in the above, one can get:

$$Q_P = C_{Q_P} K_Q \omega^2, \tag{17}$$

where, $C_{Q_P} = \frac{\rho D^5 \Omega^2_{P_{base}}}{4\pi^2 Q_{P_{base}}}$ is a constant, and the base quantities are as given in Table 2.

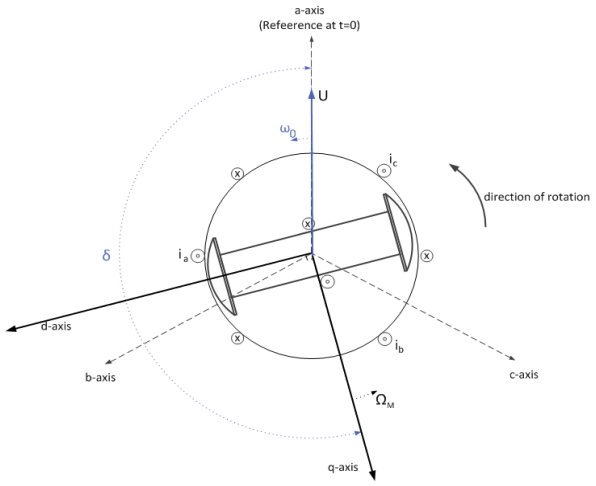

Figure 2: dq-frame in the synchronous machine and the angles involved.

2.4. Diesel Engine Model

Many mathematical models have been suggested for the diesel engines. The models vary in their complexity according to the size and properties of the engine, the purpose of the model, and the kind of the controllers used. Because they were interested in the air dynamics of the turbo-charger, the authors in [4] suggested

a sixth order model for the Diesel engine, turbo-charger and generator shaft, in which they used a first order model for the fuel actuator, and a time delay to represent the engine itself. Similarly, the following model was used in [10]:

$$\dot{\mathscr{Q}}_E = \frac{1}{\tau_E}(-\mathscr{Q}_E + K_u u_{DE}(t-\tau_D)), \tag{18}$$

where, τ_E is a time constant, u_{DE} is the input signal to control the fuel actuator, and τ_D is the time delay. In the interest of keeping the model simple, and inspired by the work in [5], we neglect the combustion delay and assume that the dynamics of the fuel actuator constitutes the essential dynamics of the engine. Thus, dividing by $Q_{E_{base}}$ given in Table 2, the model above can be described in p.u. system as [5]:

$$\dot{Q}_E = \frac{1}{\tau_E}(-Q_E + K'_u u_{DE}), \tag{19}$$

where $K'_u = \frac{K_u}{Q_{E_{base}}}$.

2.5. Frictional Torque

The main contributions to the frictional torque on the system are experienced in the side of the synchronous machine and the side of the propeller. Hence, the frictional torque can be modeled in its simplest form as a combination of two components. Linear viscous torque on the propeller shaft (see [9] for further details on frictional torque), and damping torque in the synchronous machine to compensate for neglecting the damper windings and their effect on the electrical torque produced by the machine as suggested in [8]. Thus, the frictional torque in p.u. can be written as:

$$Q_f = K_f \omega + K_D(\omega - 1), \tag{20}$$

where K_f is the propeller linear friction coefficient, and K_D is the damping torque coefficient of the synchronous machine, taking in consideration the conversion to p.u. system.

2.6. Final Model

Dividing the model in (5) by $Q_{M_{base}}$, and by using the base quantities given in Table 2, the models in (13), (17), (19), and (20) can be grouped with the model in (5) in one complete state-space model as follows:

$$\begin{aligned}
\dot{\delta} &= \omega_0(\omega - 1) \\
\dot{\omega} &= \frac{1}{2H_T}\left(Q_E - Q_M - Q_P - Q_f\right) \\
\dot{\psi}_F &= -\frac{\omega_0}{\tau_F}\frac{X_d}{X'_d}\psi_F + \frac{\omega_0}{\tau_F}\frac{X_{Fd}}{X'_d}\frac{U\cos\delta}{\omega} + \omega_0 u_F \\
\dot{Q}_E &= \frac{1}{\tau_E}\left(-Q_E + K'_u u_{DE}\right),
\end{aligned} \tag{21}$$

where H_T is the p.u. inertia constant given by:

$$H_T = \frac{1}{2}\frac{(J_M + R_{PM}^2 J_P)\Omega_{M_{base}}^2}{S_{base}} = \frac{1}{2}\frac{(J_M + R_{PM}^2 J_P)\Omega_{M_{base}}}{Q_{M_{base}}}. \tag{22}$$

The model as given above has two input controls (u_f, and u_{DE}). Usually, the output voltage U, and the propeller torque coefficient K_Q are considered as outputs and controllers are designed to regulate them. In this work, U and K_Q are modeled as uncertain parameters grouped in the vector $\boldsymbol{\theta} = [\theta_1, \theta_2]^T = [U, K_Q]^T$. The output of interest is the difference between the rotational speed and the nominal speed ($y_1 = \omega - 1$), and the main objective of the proposed controller is to regulate the shaft speed, under the disturbance imposed by the output voltage and the propeller torque coefficient. Actually, regulating the shaft speed of the system is important in order to regulate the frequency of the electrical output of the machine, since the output frequency depends on the rotational speed. Further, it was assumed that low level controllers can take care of small deviations in output frequency.

Since we are modeling the output voltage as uncertain parameter, we consider the flux linkage as another output ($y_2 = \psi_F$), because it is related to the output voltage. Further, this assumption makes the system a square 2x2 MIMO system. Thus, the rotational speed ω, and flux linkage ψ_F were assumed measurable. Let the vector $\mathbf{x} = [x_1, x_2, x_3, x_4]^T = [\delta, \omega, \psi_F, Q_E]^T$ be the state vector. Let, also, $\mathbf{u} = [u_1, u_2]^T = [u_F, u_{DE}]^T$ be the input vector. Then, the model in (21) can be rewritten as:

$$\begin{aligned}
\dot{\mathbf{x}} &= \mathbf{f}(\mathbf{x}, \boldsymbol{\theta}) + \mathbf{g}_1(\mathbf{x}, \boldsymbol{\theta})u_1 + \mathbf{g}_2(\mathbf{x}, \boldsymbol{\theta})u_2, \\
y_1 &= h_1(\mathbf{x}) \\
y_2 &= h_2(\mathbf{x})
\end{aligned} \tag{23}$$

where,

$$\mathbf{f}(\mathbf{x}, \boldsymbol{\theta}) = \begin{bmatrix} f_1(\mathbf{x}, \boldsymbol{\theta}) \\ f_2(\mathbf{x}, \boldsymbol{\theta}) \\ f_3(\mathbf{x}, \boldsymbol{\theta}) \\ f_4(\mathbf{x}, \boldsymbol{\theta}) \end{bmatrix} = \begin{bmatrix} \omega_0(x_2 - 1) \\ \frac{1}{2H_T}\left(x_4 - Q_M - Q_P - Q_f\right) \\ -\frac{\omega_0}{\tau_F}\frac{X_d}{X'_d}x_3 + \frac{\omega_0}{\tau_F}\frac{X_{Fd}}{X'_d}\frac{\theta_1 \cos x_1}{x_2} \\ -\frac{1}{\tau_E}x_4 \end{bmatrix},$$

where Q_M, Q_P, and Q_f are as given in (14), (17), and (20) respectively. Moreover,

$$\mathbf{g}_1(\mathbf{x}, \boldsymbol{\theta}) = \begin{bmatrix} 0 \\ 0 \\ \omega_0 \\ 0 \end{bmatrix}, \ \mathbf{g}_2(\mathbf{x}, \boldsymbol{\theta}) = \begin{bmatrix} 0 \\ 0 \\ 0 \\ \frac{K'_u}{\tau_E} \end{bmatrix},$$

and

$$h_1(\mathbf{x}) = x_2 - 1, \ h_2(\mathbf{x}) = x_3.$$

3. FEEDBACK LINEARIZATION

The uncertain parameters, in general, induce disturbances on the dynamical systems. The author in [11] discussed in detail the so-called *disturbance decoupling* problem, in which he discussed the conditions required to make "the feedback control law render an output y independent of some disturbance d [11]". Let us assume, for this section, that the uncertain parameter $\boldsymbol{\theta}$ is fixed. The model in (23) has a relative degree two with respect to output y_1, i.e., $r_1 = 2$. It also has relative degree one with respect to output y_2, i.e., $r_2 = 1$. Following the procedure in [11], define the characteristic matrix $\boldsymbol{\beta}(\mathbf{x}, \boldsymbol{\theta})$

as:

$$\boldsymbol{\beta} = \begin{bmatrix} L_{g_1}L_f h_1 & L_{g_2}L_f h_1 \\ L_{g_1}L_f^0 h_2 & L_{g_2}L_f^0 h_2 \end{bmatrix} = \begin{bmatrix} \omega_0 \frac{\partial f_2}{\partial x_3} & \frac{K'_u}{\tau_E}\frac{\partial f_2}{\partial x_4} \\ \omega_0 & 0 \end{bmatrix}. \tag{24}$$

Then, according to [11], since the matrix $\boldsymbol{\beta}$ is nonsingular, a diffeomorphism $(\eta, \mathbf{z}) = T(\mathbf{x}, \boldsymbol{\theta})$ exists (see Appendix. A), and is given by:

$$\begin{bmatrix} \mathbf{z} \\ \eta \end{bmatrix} = \begin{bmatrix} z_1^{(1)} \\ z_2^{(1)} \\ z_1^{(2)} \\ \eta \end{bmatrix} = \begin{bmatrix} h_1(\mathbf{x}) \\ L_f h_1 \\ h_2(\mathbf{x}) \\ \phi(\mathbf{x}, \boldsymbol{\theta}) \end{bmatrix}. \tag{25}$$

This transformation is used to linearize the system in (21). The dynamics of the new states with this transformation can be stated as:

$$\begin{bmatrix} \dot{\mathbf{z}} \\ \dot{\eta} \end{bmatrix} = \begin{bmatrix} \dot{z}_1^{(1)} \\ \dot{z}_2^{(1)} \\ \dot{z}_1^{(2)} \\ \dot{\eta} \end{bmatrix} = \begin{bmatrix} z_2 \\ L_f^2 h_1 + \beta_1(\mathbf{x}, \boldsymbol{\theta})\mathbf{u} \\ L_f h_2 + \beta_2(\mathbf{x}, \boldsymbol{\theta})\mathbf{u} \\ \dot{\phi}(\mathbf{x}, \boldsymbol{\theta}) \end{bmatrix} \tag{26}$$

where $\beta_1(\mathbf{x}, \boldsymbol{\theta})$ is the first row of $\boldsymbol{\beta}(\mathbf{x}, \boldsymbol{\theta})$, and so on. Moreover, the outputs are:

$$\begin{aligned} y_1 &= z_1^{(1)} \\ y_2 &= z_1^{(2)}. \end{aligned} \tag{27}$$

By this transformation, the new model is split into two parts; *external* part ($\mathbf{z}$), and *internal* part (η) (see [11], and [12]). The idea now is to choose a function $\phi(\mathbf{x}, \boldsymbol{\theta})$ such that the internal dynamics are independent of the control input, because this makes the stability of the system easier to be obtained as will be explained later, otherwise more complicated techniques would be required. So, letting the internal dynamics be:

$$\phi(\mathbf{x}, \boldsymbol{\theta}) = \frac{\sin x_1}{x_2}, \tag{28}$$

makes the internal dynamics $\dot{\eta}$ independent of the control input. Let the derivative of η be expressed as a function of the new variables, i.e., $\dot{\eta} = \dot{\phi}(\eta, \mathbf{z}) = \chi(\eta, \mathbf{z})$. The *zero dynamics* is defined as the internal dynamics around the zero of the linearized system, that is to say:

$$\dot{\eta} = \chi(\eta, \mathbf{z_e}), \tag{29}$$

where $\mathbf{z_e}$ is the equilibrium point of the external dynamics, which can be assumed, without loss of generality, zero. Then, according to [12], and [11] the origin of the system in (26) is asymptotically stable if the origin of (29) is asymptotically stable (see lemma 13.1 in [12] and the proof therein). Straight forward calculations show that the zero dynamics is, actually, asymptotically stable. Thus, the concern is directed now to the external dynamics only, which can be rewritten as:

$$\begin{aligned} \dot{z}_1^{(1)} &= z_2^{(1)} \\ \dot{\mathbf{z}}_\mathbf{r} &= \boldsymbol{\alpha}(\mathbf{z}, \eta) + \boldsymbol{\beta}(\mathbf{x}, \boldsymbol{\theta})\mathbf{u}, \end{aligned} \tag{30}$$

where $\mathbf{z_r} = [z_{r_1}^{(1)}, z_{r_2}^{(2)}]^T = [z_2^{(1)}, z_1^{(2)}]^T$, and $\boldsymbol{\alpha}(\mathbf{z}, \eta)$ is given by:

$$\boldsymbol{\alpha}(\mathbf{z}, \eta) = \begin{bmatrix} L_f^{r_1} h_1 \\ L_f^{r_2} h_2 \end{bmatrix} = \begin{bmatrix} L_f^2 h_1 \\ L_f h_2 \end{bmatrix}. \tag{31}$$

If the feedback control $\mathbf{u}$ is chosen such that:

$$\mathbf{u} = \boldsymbol{\beta}^{-1}(\mathbf{v} - \boldsymbol{\alpha}(\mathbf{z}, \eta)), \tag{32}$$

where $\mathbf{v} = [v_1, v_2]^T$ is an auxiliary stabilizing input control, then the external dynamics can be written as two subsystems like follows:

$$\begin{aligned} \dot{z}_1^{(1)} &= z_2^{(1)} \\ \dot{z}_2^{(1)} &= v_1, \quad \dot{z}_1^{(2)} = v_2, \end{aligned} \tag{33}$$

which is linear and controllable. Then, one can find a control law:

$$\mathbf{v} = \mathbf{K_p}\mathbf{z}, \tag{34}$$

that stabilizes the system in (33) by pole placement, for example.

4. ROBUST CONTROL

Although feedback linearization provides a good tool to deal with disturbances through disturbance decoupling, the disturbance induced by nonlinear uncertain parameters can be problematic. Firstly, the diffeomorphism $T(\mathbf{x}, \boldsymbol{\theta})$ does not provide exact linearization. Further, the equilibrium point varies due to its dependence on the parameters (see $\mathbf{x}_e$ in Appendix. B). The authors in [7] suggested an elegant way to tackle these problems by mixed H_2/H_∞ synthesis. The authors in [7] proved that if the uncertain parameter has a nominal value $\boldsymbol{\theta_0}$, and the function $\mathbf{f}(\mathbf{x}, \boldsymbol{\theta})$ can be linearized about $\boldsymbol{\theta_0}$ as:

$$\mathbf{f}(\mathbf{x}, \boldsymbol{\theta}) = \mathbf{f}_0(\mathbf{x}, \boldsymbol{\theta_0}) + \mathbf{f}_\Delta(\mathbf{x}, \boldsymbol{\theta}), \tag{35}$$

where $\mathbf{f}_0(\mathbf{x}, \boldsymbol{\theta})$ is calculated at $\boldsymbol{\theta_0}$, then the external dynamics in (26) can be rewritten, by the control law in (32) (calculated at the nominal values), as [7]:

$$\begin{aligned} \dot{z}_1^{(1)} &= z_2^{(1)} + L_{f_\Delta} h_1 \\ \dot{z}_2^{(1)} &= L_{f_\Delta} L_{f_0} h_1 + v_1 \\ \dot{z}_1^{(2)} &= L_{f_\Delta} h_2 + v_2. \end{aligned} \tag{36}$$

Now, let $\mathbf{z} = [z_1^{(1)}, z_2^{(1)}, z_1^{(2)}]^T$, $\mathbf{v} = [v_1, v_2]$, and $\mathbf{y} = [y_1, y_2]^T$. Then, by using Taylor expansion for the nonlinear disturbances in (36) and by collecting all the nonlinear terms resulting from the expansion in the matrix $\widetilde{\mathbf{A}}(\boldsymbol{\theta}, \mathbf{z})$, the authors in [7] proved that if the nonlinear perturbations are bounded such that:

$$\|\widetilde{\mathbf{A}}_i\|_2 \leq \|W_{d_i}\tilde{d}_i\|_2, \ \|\tilde{d}_i\|_2 \leq 1, \ \forall i \in \{1,2,3\}, \tag{37}$$

where $\widetilde{\mathbf{A}}_i$ is the ith row of the matrix, $\tilde{d}_i \in \mathscr{L}_2[0,\infty)$, and W_{d_i} are linear weights. Then, the model in (36) can be rewritten as [7]:

$$\dot{\mathbf{z}} = \mathbf{A}(\boldsymbol{\theta})\mathbf{z} + \mathbf{W}_d\tilde{\mathbf{d}} + \mathbf{B}(\boldsymbol{\theta})\mathbf{v}, \tag{38}$$

where $\mathbf{W}_d = \mathrm{diag}(W_{d_1}, W_{d_2}, W_{d_3})$, and $\tilde{\mathbf{d}} = [\tilde{d}_1, \tilde{d}_2, \tilde{d}_3]^T$. Mimicking the procedure above, one can obtain

$\mathbf{f}_\Delta(\mathbf{x},\boldsymbol{\theta})$ to be:

$$\mathbf{f}_\Delta(\mathbf{x},\boldsymbol{\theta}) = \begin{bmatrix} 0 \\ \frac{-1}{2H_T}\left[\frac{\partial Q_M}{\partial \theta_1}|_{\theta_1=\theta_{0_1}}\Delta\theta_1 + \frac{\partial Q_P}{\partial \theta_2}|_{\theta_2=\theta_{0_2}}\Delta\theta_2\right] \\ \frac{\omega_0}{\tau_F}\frac{X_{Fd}}{X'_d}\frac{\cos x_1}{x_2}\Delta\theta_1 \\ 0 \end{bmatrix},$$

$$\mathbf{A} = \begin{bmatrix} D_1\Delta\theta_1 + 2C_{Q_P}\Delta\theta_2 & 1 & D_2\Delta\theta_1 \\ \widetilde{D}_1\Delta\theta_1 + \widetilde{C}_{Q_P}\Delta\theta_2 & 0 & \widetilde{D}_2\Delta\theta_1 \\ D_3\Delta\theta_1 & 0 & 0 \end{bmatrix}, \quad (39)$$

and

$$\mathbf{B}(\boldsymbol{\theta}) = \begin{bmatrix} 0 & 0 \\ 1 & 0 \\ 0 & 1 \end{bmatrix}, \mathbf{C} = \begin{bmatrix} 1 & 0 & 0 \\ 0 & 0 & 1 \end{bmatrix}, \quad (40)$$

where $\Delta\theta_1 = \theta_1 - \theta_{0_1}$ and so on, the parameters D_1, D_2, D_3, $\widetilde{D}_1$, $\widetilde{D}_2$, and $\widetilde{C}_{Q_P}$ are as given in Appendix. B.
Finally, following the procedure to design a mixed H_2/H_∞ controller (see e.g., [7]), define:

$$\begin{aligned} \dot{\mathbf{z}} &= \mathbf{A}(\boldsymbol{\theta})\mathbf{z} + \mathbf{W}_d\tilde{\mathbf{d}} + \mathbf{B}(\boldsymbol{\theta})\mathbf{v} \\ \mathbf{Z}_\infty &= \mathbf{E}_1\mathbf{z} + \mathbf{F}_{11}\tilde{\mathbf{d}} + \mathbf{F}_{12}\mathbf{v} \\ \mathbf{Z}_2 &= \mathbf{E}_2\mathbf{z} + \mathbf{F}_{22}\mathbf{v}. \end{aligned} \quad (41)$$

Now a feedback law

$$\mathbf{v} = \mathbf{K_m}\mathbf{z}, \quad (42)$$

that stabilizes the system in (41), can be obtained by using the *Linear Matrix Inequality* (LMI) toolbox in MATLAB. This control law aims to minimize the combined objective of $\|.\|_2$, and $\|.\|_\infty$ of the transfer functions of the disturbance to the defined output signals $\mathbf{Z}_2$, and $\mathbf{Z}_\infty$. Straight-forward calculations from (32) show that the control law $\mathbf{u}$ can be written as:

$$\mathbf{u} = \begin{bmatrix} 0 & \frac{1}{\omega_0} \\ \frac{2H_T\tau_E}{K'_u} & -\frac{\tau_E X_{Fd}\theta_1}{K'_u X_F X'_d}\frac{\sin x_1}{x_2} \end{bmatrix} \begin{bmatrix} v_1 - L_{f_0}^2 h_1 \\ v_2 - L_{f_0} h_2 \end{bmatrix}. \quad (43)$$

5. SIMULATIONS AND RESULTS

The parameters used in the simulations are listed in Tables 1 and 2. By using the values listed in the tables, one can obtain $C_{Q_P} = 16.4$, and $H_T = 0.7305\text{s}^2$. The system in (21) was simulated in MATLAB/SIMULINK. Both control gains were found, $\mathbf{K_p}$ in (34) was found by pole placement, and $\mathbf{K_m}$ in (42) was found by the mixed H_2/H_∞ synthesis technique in (41) by using the LMI toolbox. Actually, high gains are required to stabilize the slow dynamics. To elucidate, the control law $\mathbf{u}$ in (43) cancels the nonlinear terms and stabilizes the states, but the inertia constant H_t is large compared to the diesel engine time constant τ_E, so high gains are required. Hence, the weighting matrices $\mathbf{W}_d$,$\mathbf{E}_1$, $\mathbf{E}_2$, $\mathbf{F}_{11}$, $\mathbf{F}_{12}$, and $\mathbf{F}_{22}$ in (41) were chosen to be:

$$\mathbf{W}_d = \begin{bmatrix} 1 & 0 & 0 \\ 0 & 2 & 0 \\ 0 & 0 & 2.5 \end{bmatrix}, \mathbf{E}_1 = \mathbf{E}_2 = \begin{bmatrix} 0.005 & 0 & 0 \\ 0 & 1.5 & 0 \\ 0 & 0 & 2.85 \end{bmatrix},$$

$$\mathbf{F}_{11} = \begin{bmatrix} 0.1 & 0 & 0 \\ 0 & 0.2 & 0 \\ 0 & 0 & 0.5 \end{bmatrix}, \mathbf{F}_{12} = \mathbf{F}_{22} = \begin{bmatrix} 0 & 0 \\ 0 & 0 \\ 1 & 1 \end{bmatrix},$$

Table 1: The Parameters

Electrical		Mechanical	
Quantity	Value	Quantity	Value
X_d (p.u.)	2	ρ (Kg/m^3)	1000
X'_d (p.u.)	0.25	D (m)	3.0
X_q (p.u.)	1	τ_E (s)	0.01
X_{Fd} (p.u.)	1.8	K'_u (p.u.)	1
X_F (p.u.)	2.1	K_f (p.u.)	0.1
τ_F (s)	3.0	K_D (p.u.)	155
ω_0 (rad/s)	377	J_M (Kg.m^2)	270
p	6	J_P (Kg.m^2)	300

Table 2: The Base Quantities

Quantity	Expression	Value
$\Omega_{M_{base}}$ (rad/s)	$\omega_0/(\frac{p}{2})$	125.66
$\Omega_{E_{base}}$ (rad/s)		80
$\Omega_{P_{base}}$ (rad/s)		20
U_{base} (V)		360
I_{base} (A)		5555
S_{base} (kVA)	$\frac{3}{2}U_{base}I_{base}$	3000
$Q_{M_{base}}$ (kN.m)	$\frac{S_{base}}{\Omega_{M_{base}}}$	23.9
$Q_{E_{base}}$ (kN.m)	$\frac{S_{base}}{\Omega_{E_{base}}}$	37.5
$Q_{P_{base}}$ (kN.m)	$\frac{S_{base}}{\Omega_{P_{base}}}$	150

and the gain $\mathbf{K_m}$ was obtained to be:

$$\mathbf{K_m} = \begin{bmatrix} -4.3905 & -0.0141 & 0.3769 \\ 4.3905 & 0.0141 & -0.3769 \end{bmatrix} \times 10^6,$$

For the gain $\mathbf{K_p}$, if the gain is not high enough the control law can not stabilize the system. On the other hand, raising the control gain could lead to excessive control action. The best results were found when the poles were placed at -180, -260, and -130 for the three states of the linearized model in (33). The gain $\mathbf{K_p}$ was obtained to be:

$$\mathbf{K_p} = \begin{bmatrix} -46800 & -440 & 0 \\ 0 & 0 & -130 \end{bmatrix}.$$

The control law was applied to the model with arbitrary initial values twice, one with the gain $\mathbf{K_p}$, and one with the gain $\mathbf{K_m}$ for comparison. The nominal values of the uncertain parameters were assumed $\theta_{0_1} = 1$, and $\theta_{0_2} = 0.008$. The simulations were run in two cases assumed for the uncertainties of the parameters θ_1, and θ_2 as shown in Table3. The trajectories of the output signals ψ_F, and ω are shown in Fig. 3 and Fig. 4 for cases one and two, respectively. We can see from Fig. 3 that both output trajectories reach the equilibrium by both control gains, because the uncertainties assumed in this case are not large. On the other hand, Fig. 4 shows that control gain obtained from H_2/H_∞ synthesis ($\mathbf{K_m}$) drives the output to the steady state more quickly than

Table 3: The Uncertain parameters

	$\Delta\theta_1$	$\Delta\theta_2$
Case I	2%	5%
Case II	20%	50%

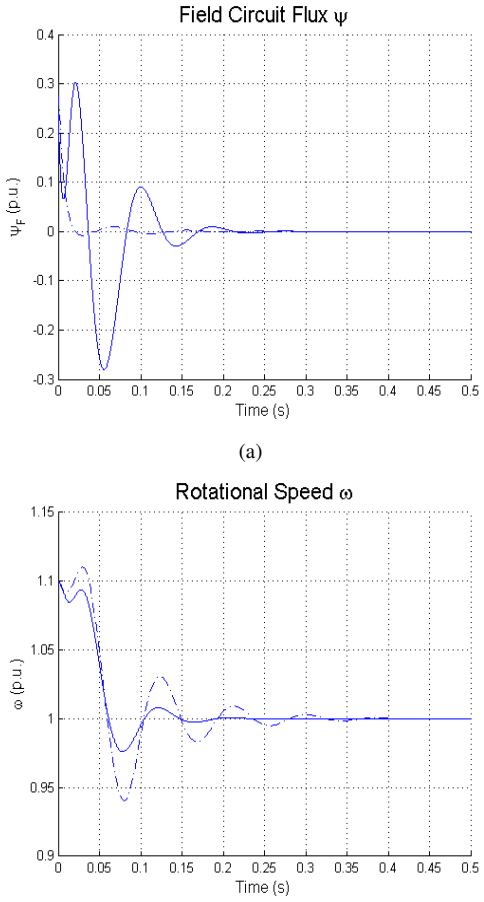

Figure 3: Comparison of the output trajectories: (a) The field circuit flux (ψ_F), and (b) Rotational speed (ω), obtained by the two strategies: H_2/H_∞ synthesis (solid), and pole placement (dashed) when the the uncertainties of the two parameters $\Delta\theta_1 = 2\%$, and $\Delta\theta_2 = 5\%$.

the other gain $\mathbf{K_p}$, for the same chosen poles. One can advocate that changing the gain $\mathbf{K_p}$ may give better results. The problem with the former argument is that the gain $\mathbf{K_p}$ should be varied for every range of uncertainties. Whereas, the gain $\mathbf{K_m}$ could stabilize the system for different uncertainty ranges. Because the propeller torque coefficient K_Q, which was modeled as uncertain parameter, varies significantly in reality due to several factors such as weather condition, ship speed and sea condition, H_2/H_∞ robust controller is recommended for this model.

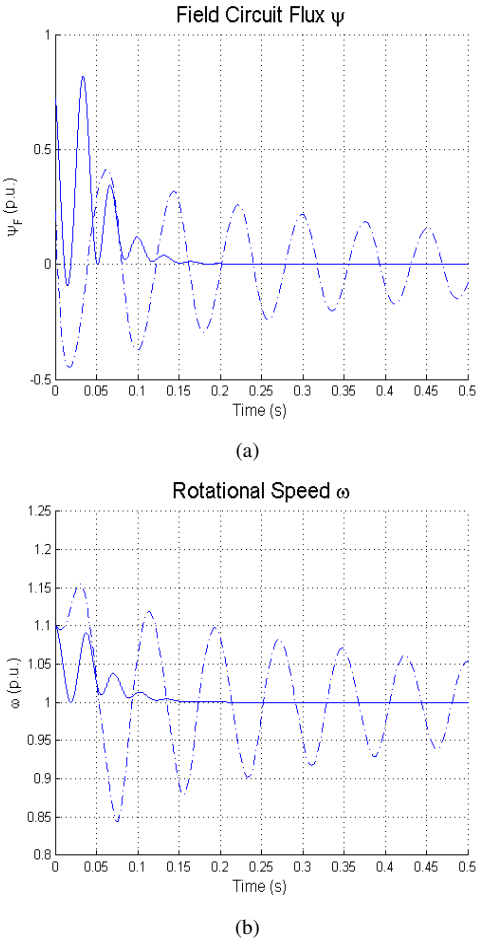

Figure 4: Comparison of the output trajectories: (a) The field circuit flux (ψ_F), and (b) Rotational speed (ω), obtained by the two strategies: H_2/H_∞ synthesis (solid), and pole placement (dashed) when the the uncertainties of the two parameters $\Delta\theta_1 = 20\%$, and $\Delta\theta_2 = 50\%$.

6. FUTURE WORK

In this work, we concentrated on the operation of the described system in one mode, PTO. It is of interest to apply the proposed controllers on the system in the other mode, i.e., PTI. Then, a hybrid control strategy can be applied to smoothen the transition between the modes, and/or decide the optimal mode of operation regarding fuel consumption. Also, work on making less restrictive assumptions in the modeling is ongoing.

7. CONCLUSIONS

In this paper, a model was proposed for Gensets, that comprise a medium-size diesel engine driving a synchronous machine to generate electric power, and a propeller, simultaneously. The output voltage of the synchronous machine, and the propeller torque coefficient were modeled as uncertain parameters. A feedback linearization was performed. Then, two nonlinear

control laws were proposed to regulate the shaft rotational speed, by pole placement, and by mixed H_2/H_∞ synthesis. The simulations showed that the proposed controllers could stabilize the shaft speed. In addition, we showed that the mixed H_2/H_∞ controller could stabilize the shaft speed more quickly than the pole placement controller, regardless of how much the output voltage and/or the propeller torque coefficient may vary.

References

[1] L. Guzzella, and A. Amstutz, "Control of Diesel Engines," *IEEE Control Systems*, vol. 18, issue 5, pp. 53-71, 1998.

[2] M. Blanke, K. P. Lindegaard, and T. I. Fossen, "Dynamic Model for Thrust Generation of Marine Propellers," *IFAC Conference of Maneuvering and Control of Marine craft (MCMC)*, pp. 363-368, 2000.

[3] A. J. Sørensen, and Ø. Smogeli, "Torque and Power Control of Electrically driven Marine Propellers," *Control Engineering Practice*, vol. 17, no. 9, pp. 10531064, 2009.

[4] S. Roy, O. P. Malik, and G. S. Hope, "Adaptive Control Of Speed And Equivalence Ratio Dynamics of a Diesel Driven Power-Plant," *IEEE Transactions on Energy Conversion*, vol. 8, no. 1, pp. 13-19, 1993.

[5] J. F. Hansen, A. K. Ådnanes, and T. I. Fossen, "Mathematical Modeling of Diesel-Electric Propulsion Systems for Marine Vessels," *Mathematical and Computer Modeling of Dynamical Systems*, vol. 7, no. 1, pp. 1-33, 2001.

[6] M. L. Huang, "Robust Control Research of Chaos Phenomenon for Diesel-Generator Set on Parallel Connection," *Applications of Nonlinear Control, Intec.*, 2012.

[7] S. N. Kolavennu, S. Palanki, and J. C. Cockburn, "Robust controller design for multivariable nonlinear systems via multi-model H_2/H_∞ synthesis," *Chemical Engineering Science*, vol. 56, pp. 4339-4349, 2001.

[8] P. Kundur, *Power System Stability And Control*, McGraw-Hill, 1994.

[9] L. Pivano, T. A. Johansen, Ø. N. Smogeli, and T. I. Fossen, "Nonlinear Thrust Controller for Marine Propellers in Four-Quadrant Operations," *Proceedings of the American Control Conference*, pp. 900-905, 2007.

[10] M. Torres, and L. A. C. Lopes, "Inverter-Based Diesel Generator Emulator for the Study of Frequency Variations in a Laboratory-Scale Autonomous Power System," *Energy and Power Engineering (EPE)*, vol. 5, pp. 274-283, 2013.

[11] A. Isidori, *Nonlinear Control Systems*, Springer-Verlag, Berlin, 2nd edition, 1989.

[12] H. K. Khalil, *Nonlinear Systems*, Prentice Hall, New Jersey, 3rd edition, 2002.

A. Transformation

The transformation $T^{-1}(\mathbf{z},\eta)$ was found to be:

$$T^{-1}(\mathbf{z},\eta)=\begin{bmatrix} \arcsin(\eta(z_1^{(1)}+1)) \\ z_1^{(1)}+1 \\ z_1^{(2)} \\ C_{Q_P}\theta_2(z_1^{(1)}+1)^2+(K_f+K_D)z_1^{(1)}+\dots \\ K_f+(\frac{1}{X_q}-\frac{1}{X'_d})\theta_1^2\eta\sqrt{\frac{1}{(z_1^{(1)}+1)^2}-\eta^2}+\dots \\ 2H_T z_2^{(1)}+\frac{X_{Fd}}{X_F X'_d}\theta_1 z_1^{(2)}\eta \end{bmatrix}.$$

B. Parameters

The parameters D_1, D_2, D_3, $\widetilde{D}_1$, $\widetilde{D}_2$, and $\widetilde{C}_{Q_P}$ are as follows:

$$\begin{aligned} D_1 &= \frac{\theta_{0_1}\eta_0}{H_T\sqrt{1-\eta_0^2}}(\frac{1}{X_q}-\frac{1}{X'_d}) \\ D_2 &= -\frac{X_{Fd}\eta_0}{2H_T X_F X'_d} \\ D_3 &= -\frac{\omega_0 X_{Fd}}{\tau_F X'_d\sqrt{1-\eta_0^2}} \\ \widetilde{D}_1 &= \frac{-1}{2H_T}(K_f+K_D)D_1 \\ \widetilde{D}_2 &= \frac{-1}{2H_T}(K_f+K_D)D_2 \\ \widetilde{C}_{Q_P} &= \frac{-1}{H_T}(K_f+K_D)C_{Q_P} \\ \eta_0 &= \frac{\sin(x_{e_1})}{x_{e_2}}, \end{aligned}$$

where x_e is the equilibrium point given by:

$$\mathbf{x}_e=\begin{bmatrix} \frac{1}{2}\arcsin\Big(\frac{-2(K_f+C_{Q_P}\theta_2)}{\theta_1^2\left[(\frac{1}{X_q}-\frac{1}{X'_d})+(\frac{X_{Fd}}{X_F})^2\frac{1}{X_d X'_d}\right]}\Big)\pm n\pi \\ 1 \\ \frac{X_{Fd}}{X_d}\theta_1\cos(x_{e_1}) \\ 0 \end{bmatrix}.$$